

See discussions, stats, and author profiles for this publication at: <https://www.researchgate.net/publication/320085997>

Modelling rainfall interception by urban trees

Article in *Canadian Water Resources Journal* · September 2017

DOI: 10.1080/07011784.2017.1375865

CITATION

1

READS

341

4 authors, including:



[Les M Lavkulich](#)

University of British Columbia - Vancouver

147 PUBLICATIONS 2,165 CITATIONS

[SEE PROFILE](#)

Some of the authors of this publication are also working on these related projects:



UBC Forest Ecosystems [View project](#)



Modelling rainfall interception by urban trees

Jie Ying Huang, T.A. Black, R.S. Jassal & L.M. Les Lavkulich

To cite this article: Jie Ying Huang, T.A. Black, R.S. Jassal & L.M. Les Lavkulich (2017): Modelling rainfall interception by urban trees, Canadian Water Resources Journal / Revue canadienne des ressources hydriques, DOI: [10.1080/07011784.2017.1375865](https://doi.org/10.1080/07011784.2017.1375865)

To link to this article: <http://dx.doi.org/10.1080/07011784.2017.1375865>



Published online: 28 Sep 2017.



Submit your article to this journal [↗](#)



Article views: 15



View related articles [↗](#)



View Crossmark data [↗](#)

Modelling rainfall interception by urban trees

Jie Ying Huang, T.A. Black, R.S. Jassal and L.M. Les Lavkulich*

Faculty of Land and Food System, University of British Columbia, Vancouver, Canada

(Received 24 February 2017; accepted 31 August 2017)

Trees in the urban environment have significant effects on the hydrological cycle by aiding in the reduction of stormwater runoff through rainfall interception. Factors such as wind exposure, relative humidity and leaf area index in the urban environment differ from those in a forest and affect the processes occurring within the canopy of conifers and deciduous tree species differently. This study focused on the interception losses of trees in an urban setting with a view to providing some information on tree selection in urban environments. An analytical model was formulated based on a rainfall interception model developed for sparse canopy forests and preliminary data on water losses from tree canopy interception. The model was validated using empirical data, and an assessment of the performance of the model for four deciduous tree species (white oak, Norway maple, green ash and *Prunus* sp.). Model-calculated values of interception losses and throughfall were congruent with measured empirical values. Sensitivity analysis with respect to model parameter values revealed that evaporation and rainfall rates were the most sensitive parameters for model output. The ratio of evaporation rate to rainfall rate used in the model was identified as the most dynamic parameter. To measure independently the two components requires further analysis, and a more reliable measurement of leaf area index.

Les arbres en milieu urbain ont des effets significatifs sur le cycle hydrologique de par leurs capacités à réduire le ruissellement des eaux pluviales lorsqu'ils interceptent les précipitations. Les facteurs tels que l'exposition au vent, l'humidité relative ou l'indice de surface foliaire diffèrent en milieu urbain et forestier et affectent différemment les processus se produisant au niveau de la canopée des espèces de conifères et décidus. Cette étude s'est concentrée sur les processus d'interception des arbres en milieu urbain afin d'aider à la sélection des arbres dans ce milieu. Un modèle analytique a été développé en se basant sur le modèle d'interception des précipitations élaboré pour des forêts à canopées clairsemées et sur des données préliminaires sur les pertes d'eau résultant de l'interception au niveau de la canopée. Le modèle a été validé par des données empiriques et part une évaluation des performances du modèle pour quatre espèces d'arbres (le chêne blanc, l'érable de Norvège, le frêne vert et une espèce du genre *Prunus*). Les résultats du modèle d'interception des pertes et du pluviométrisme ont été en accord avec les mesures empiriques. L'analyse de sensibilité a révélé que les taux d'évaporation et de précipitation ainsi que le stockage de l'eau au niveau du couvert étaient les paramètres les plus sensibles pour la performance du modèle. Le ratio taux d'évaporation/taux de précipitation utilisé dans le modèle a été identifié comme le paramètre le plus dynamique.

List of symbols and abbreviations

BAI (B)	= bark area index of a single tree (m^2 bark m^{-2} ground)
LAI (L)	= leaf area index of a single tree (m^2 leaves m^{-2} ground)
c	= canopy cover (dimensionless)
c_p	= specific heat of air
\bar{E}_c	= mean rate of evaporation from the tree during saturated conditions (mm h^{-1})
\bar{E}	= mean rate of evaporation at forest stand during saturated conditions (mm h^{-1})
e_a	= actual vapour pressure of air (kPa)
e_s	= saturation vapour pressure (kPa)
g_{bV}	= aerodynamic conductance for water vapour integrated over the distance between the surface of the foliage and the adjacent air (m s^{-1})
I	= interception loss (mm)
I_c	= interception loss from canopy for events $P_G < P_g$ (mm)
I_s	= interception loss from canopy for events $P_G \geq P_g$ (mm)
I_t	= interception loss from trunk for events $P_G < P_g$ (mm)
I_{ts}	= interception loss from trunk for events $P_G \geq P_g$ (mm)
k	= radiation extinction coefficient (dimensionless)

*Corresponding author: E-mail: lml@mail.ubc.ca

p	= free throughfall proportion (dimensionless)
p_d	= drainage partitioning coefficient
P_G	= gross rainfall for a single rainfall event (mm)
P_g	= gross rainfall required to saturate the canopy (mm)
P'_g	= amount of rainfall required to saturate the trunk (mm)
P_n	= net rainfall below the canopy (mm)
\bar{R}	= mean rate of rainfall during saturated canopy conditions (mm h^{-1})
RH	= relative humidity of the air (%)
S	= saturation storage of the crown (mm)
S_t	= saturation storage of the trunk (mm)
S_L	= specific leaf storage (mm)
S_b	= specific bark surface storage (mm)
T	= throughfall (free throughfall, canopy drip and stemflow during the entire rainfall event) ($= P_n$) (mm)
T_n	= free throughfall (mm)
T_a	= air temperature ($^{\circ}\text{C}$)
T_w	= air wet bulb temperature ($^{\circ}\text{C}$)
t	= duration of rainfall event (h)
u	= wind speed (m s^{-1})
ρ	= density of air (kg m^{-3})
γ	= psychrometric constant ($\text{kPa } ^{\circ}\text{C}^{-1}$)
λ	= latent heat of vaporization of water (kJ kg^{-1})
ε	= fraction of evaporation rate from the saturated tree that comes from the trunks

Introduction

Urban trees play critical roles in regulating hydrological cycles and affecting surface water in the urban environment (Xiao et al. 2003; Wang et al. 2008; Livesley et al. 2016). Urban trees have been considered a tool to help reduce stormwater runoff generation by intercepting, infiltrating and evaporating significant amounts of rainwater. New urban developments often lead to an increase of impervious surface areas, which results in an increasing amount of stormwater runoff. Strategic tree planting and maintenance of existing street trees can decrease stormwater runoff. It has been estimated that the annual benefit of avoided stormwater treatment and flood control costs associated with rainfall interception of urban trees in California was \$41.5 million US dollars (McPherson et al. 2016). In addition, the annual value per street tree of services was reported from \$3.78 (McPherson et al. 2002) to as high as \$29.90 (McPherson et al. 2016) in some cities in the United States. In addition to regulating the urban hydrological cycle, urban trees also benefit the environment in terms of sequestering carbon, improving air quality, and reducing energy consumption by providing shade (Livesley et al. 2016). A recent survey in the State of California found that the average annual per-tree management expenditure is US \$19.00 and the benefit is \$110.63; thus, a value of \$5.82 in benefit is returned for every \$1 spent (McPherson et al. 2016). A similar return on urban tree investment was reported as \$5.60 in New York (Peper et al. 2007). Trees are becoming key components of urban green infrastructure.

Rainfall is intercepted by the tree crown surface, and some raindrops directly pass through gaps between leaves and the stems, reaching the ground as free throughfall. Rainwater intercepted by tree leaves and branches is temporarily stored on leaf and bark surfaces (Xiao et al. 2003). Eventually, this stored water evaporates into the atmosphere, or flows down the trunk to the ground as stemflow, or drips from the leaf surfaces to the ground (Xiao et al. 2003). Compared to other benefits associated with urban trees, relatively few investigations have focused on the influence of urban trees on rainfall interception and stormwater runoff reduction. Many previous studies have investigated interception loss in continuous trees stands or forest communities (Bryant et al. 2005; Murakami 2007; Pereira et al. 2009a), while only a few studies have looked at interception loss of trees in the urban environment (Xiao et al. 2000; Asadian et al. 2009).

Trees in urban areas are exposed to an environment different to that of trees in the forest (Xiao et al. 2000; Véliz-Chávez et al. 2014). The factors affecting rainfall interception of trees in urban environments, such as wind speed, spatial rainfall distribution, and leaf area index (LAI) are different from those in natural forests (Xiao et al. 2000). For example, the storage capacity of the tree crown will be affected by the LAI, which is the leaf area (usually one-sided leaf area) per unit ground area. LAI differs among species and seasons and has significant effects on processes such as photosynthesis, respiration, rainfall interception and evaporation (Deguchi et al. 2006; Šraj et al. 2008). Deciduous trees lose their leaves

during winter, thus allowing a significant amount of throughfall, while conifers intercept considerable precipitation during the winter because they retain most of their leaves (Asadian et al. 2009). It has been reported that the annual average canopy interception for *Pseudotsuga menziesii* (Douglas-fir) and *Thuja plicata* (western redcedar) in the District of North Vancouver, British Columbia, was 49.1 and 60.9%, respectively (Asadian et al. 2009), and interception by street and park trees in Santa Monica, California, ranged from 15.3% for a small *Jacaranda mimosifolia* to 66.5% for a mature *Tristania conferta* (Xiao et al. 2003).

Quantifying the potential rainfall interception by different species in the urban environment is important because it provides information to assist in tree selection and the decision-making process for the design of new urban developments, as well as to determine the potential monetary values associated with different tree species. Studies that differentiate the amount of rainfall interception by different species are relatively few. Thus, it is important to adapt previous studies of interception loss in forest communities to allow a better understanding of the interception process for tree species in the urban environment, as well as to quantify the potential performance of different tree species.

This study is aimed at providing an analytical model of rainwater interception by a selection of common urban trees in Metro Vancouver, given annual climatic conditions and tree characteristics. This model builds upon several key studies: (1) a previous rainfall interception model that was applied in sparse forests stands (Gash et al. 1995; Valente et al. 1997; Pereira et al. 2009b), and (2) field research that investigated the interception loss of a variety of tree species in the District of North Vancouver (Asadian et al. 2009). The model outputs and interface are designed to inform and enhance decision support tools, such as the Water Balance Model Express (2016), used in the development of stormwater management plans and permit applications associated with urban development projects in the District of North Vancouver, and potentially other municipalities. Specific goals of this study include: (1) developing the rainfall interception model with different approaches of obtaining model parameters; (2) evaluating the performance of the model and sensitivity to major model parameters; and (3) investigating the seasonal rainfall interception variability of four deciduous tree species.

Theory

This work is based on the modified version of the Gash model (Gash et al. 1995; Valente et al. 1997; Pereira et al. 2009b) developed for sparse forest canopies. The original Gash analytical model (1979) is a storm-based interception model assuming rainfall is a succession of

discrete storms, separated by periods long enough to allow the canopy to dry completely. Each of the discrete storms comprises three distinct phases: (1) the canopy wets up from the beginning of rainfall until saturation is reached; (2) the canopy is completely saturated while rainfall continues; and (3) following the cessation of rainfall, the trunks and the canopy dry out completely (Gash 1979). Taking the sparseness of the canopy into consideration, the revised Gash model (Gash et al. 1995; Valente et al. 1997; Pereira et al. 2009b) scales the mean evaporation rate during a rainfall event and other model parameters to the proportion of canopy cover, and assumes no trunk storage before canopy saturation is reached. Valente et al. (1997) made a further modification by replacing the mean evaporation from canopy, \bar{E}_c , with $(1 - \varepsilon)\bar{E}_c$, where ε is a constant describing the evaporation rate from the saturated trunks as a proportion of that from the saturated canopy (Valente et al. 1997; Price et al. 2003). Valente et al. (1997) found similar values of ε in two contrasting stands, 0.024 in a *Pinus pinaster* stand and 0.022 in a *Eucalyptus globulus* stand, indicating that ε does not vary significantly in different forest stands (Price et al. 2003). Accordingly, a value of 0.023 for ε was used in the model calculations. The revised Gash model used the Penman–Monteith model in estimating the evaporation rate, which may be questionable especially in spatially non-homogeneous vegetation such as very sparse forests (Pereira et al. 2009b). Considering the urban context in this study, an alternative method of estimating evaporation rate suggested by Pereira et al. (2009b) was used. The storage associated with branches and trunks was considered in total rainwater storage capacity (S) by applying documented branch and stem storage capacities, and surface area for each tree species as described earlier (Liu 1998; Xiao et al. 2016).

Model theory

By definition, interception is the part of rain that falls on the vegetation and evaporates without reaching the ground, and is expressed as $I = P_G - T$, where I is the interception (mm), P_G is the gross (i.e. above-canopy) rainfall (mm), and T is the total throughfall (i.e. the sum of free throughfall, canopy drip and stemflow (mm)), which is the net rainfall beneath the canopy (P_n) (Klaassen et al. 1995).

Free throughfall is the part of P_G that directly reaches the ground without touching the leaves and branches. The ratio of free throughfall to P_G is called the free or direct throughfall coefficient (p). Thus, T will increase approximately linearly with P_G until the canopy is saturated (Figure 1). For a single rainfall event, the amount of free throughfall that occurs before saturation is given by (Gash 1979):

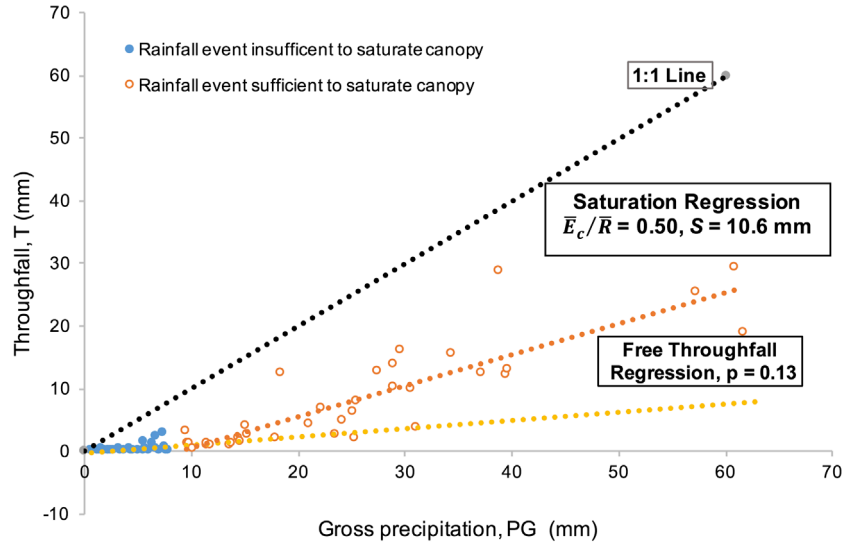


Figure 1. Example plot of data used to determine the free throughfall coefficient (p) and the saturation storage capacity (S), and the evaporation rate to rainfall rate ratio (\bar{E}_c/\bar{R}). The data shown are the throughfall for a single Douglas-fir tree, obtained by Asadian and Weiler (2009).

$$T = pP_G, P_G < P_g \quad (1)$$

where P_g is the gross rainfall required to saturate the canopy; the remaining part ($1 - p$) may be temporarily stored on the canopy, evaporated into the atmosphere or drained to the forest floor (Klaasen et al. 1995). The parameter p is often assumed to equal to one minus the canopy cover (c), which is a measure of the fraction of the landscape covered by vegetation (Gash et al. 1995).

After the accumulated P_G reaches P_g , the slope of the T vs. P_G plot is larger than before saturation but will be < 1 , because evaporation is occurring during the rainfall; otherwise, the slope will be unity if there is no evaporation (Link et al. 2004). Thus, for a rainfall P_G greater than P_g , T in a single rainfall event is given as

$$T = pP_g + (1 - p) \left(1 - \frac{\bar{E}_c}{\bar{R}} \right) (P_G - P_g), P_G \geq P_g \quad (2)$$

where \bar{E}_c and \bar{R} are average evaporation and rainfall rates (mm h^{-1}) when the canopy is saturated.

By plotting the relationship between T and P_G , the main parameters of the model to be used in this study can be estimated using the Leyton et al. (1967) method. The throughfall coefficient p is the slope of the free throughfall vs. P_G regression line in Figure 1, \bar{E}_c/\bar{R} is determined by the slope of saturation throughfall versus P_G regression line, and S is determined as $(1 - p)P_g$ (Figure 1).

The T in Figure 1 is the total throughfall, which includes the sum of free throughfall, canopy drip and

stemflow (mm). Stemflow is generally assumed to be negligible ($< 5\%$ of precipitation) compared to throughfall as observed in many interception loss studies (e.g. Link et al. 2004; Šraj et al. 2008; Asadian et al. 2009; Pereira et al. 2009a). However, more recent literature on stemflow studies emphasizes the importance of stemflow in estimating interception loss, especially for some deciduous tree species in urban settings (Carlyle-Moses et al. 2015; Schooling et al. 2015). In the revised Gash model, the partitioning of canopy drainage into the trunk is also eliminated from the total amount of free throughfall by introducing the drainage partitioning coefficient (p_d) (Valente et al. 1997). To separate stemflow and canopy drip from throughfall, the amount of free throughfall, T_n , is used. In this case, for a rainfall P_G greater than P_g , T_n in a single rainfall event is given as (Valente et al. 1997):

$$T_n = pP_g + (1 - p_d)(1 - p) \left(1 - \frac{(1 - \varepsilon)\bar{E}_c}{\bar{R}} \right) (P_G - P_g), P_G \geq P_g \quad (3)$$

Interception calculation

The different components of rainfall interception were calculated from Gash et al. (1995) and Valente et al. (1997), as follows:

For m small storms insufficient to saturate the canopy (i.e. $P_G < P_g$, which is defined below), the amount of interception (I_c) was computed as:

$$I_c = (1 - p) \sum_{j=1}^m P_{G,j} \quad (4)$$

For n large storms sufficient to saturate the canopy (i.e. $P_G \geq P_g$):

$$I_s = c \left[n(1 - p)P_g + \frac{(1 - \varepsilon)\bar{E}_c}{\bar{R}} \sum_{j=1}^n (P_{G,j} - P_g) \right] \quad (5)$$

For q storms that saturate the trunks (i.e. $P_G \geq P'_g$, which is defined below):

$$I_{ts} = qS_t \quad (6)$$

where S_t is trunk storage capacity.

For $n - q$ storms that do not saturate the trunks (i.e. $P_G < P'_g$):

$$I_t = p_d c \left[1 - \frac{(1 - \varepsilon)\bar{E}_c}{\bar{R}} \right] \sum_{j=1}^{n-q} (P_{G,j} - P_g) \quad (7)$$

Therefore, the total interception loss is:

$$I = I_c + I_s + I_{ts} + I_t \quad (8)$$

Assuming no water drips from the canopy before saturation, the mean amount of rainfall required to saturate the canopy (P_g) and the mean amount of rainfall required to saturate the trunk (P'_g) are given by:

$$P_g = -\frac{\bar{R}}{(1 - \varepsilon)\bar{E}_c} \frac{S}{c} \ln \left[1 - \frac{(1 - \varepsilon)\bar{E}_c}{\bar{R}} \right] \quad (9)$$

$$P'_g = -\frac{\bar{R}}{\bar{R} - (1 - \varepsilon)\bar{E}_c} \frac{S_t}{p_d c} + P_g \quad (10)$$

Methods

Study site

This project focuses on the District of North Vancouver (DNV), which is located within the Regional District of Metro Vancouver (Figure 2). The elevation of urban areas in the DNV ranges from below mean sea level to 200 m above sea level. The DNV, which is located in the Coastal Western Hemlock Biogeoclimatic Zone, is surrounded by the Coast Mountains to the North, Burrard Inlet to the south, Capilano River to the west and Indian Arm to the east. The annual precipitation ranges from 1200 to 3000 mm depending on the elevation, and the average annual temperature is about 10°C at sea level. A rainfall interception model will benefit new urban developments by providing critical information to help urban planners and stormwater managers. The outcome of the model is intended to support the implementation of rainwater management plans in the District of North Vancouver.

Derivation of parameters and data requirements

When no throughfall measurements are made, this analysis may be used to obtain each of the model parameters by the following approaches. The value of \bar{E}_c was calculated using the water vapour diffusion equation as used by Pereira et al. (2009b) with the required inputs of meteorological data:

$$\bar{E}_c = \frac{\rho c_p g_{bV}}{\lambda \gamma} [e_s(T_w) - e_a] \quad (11)$$

where ρ is the density of air (kg m^{-3}), c_p is the specific heat of air at constant pressure (kJ kg^{-1}), λ is the latent heat of vaporization of water (kJ kg^{-1}), γ is the psychrometric constant ($\text{kPa } ^\circ\text{C}^{-1}$), e_a is the vapour pressure of air (kPa), and $e_s(T_w)$ is the saturation vapour pressure (kPa) at the air wet bulb temperature (T_w), which has been shown to be approximately equal to tree crown surface temperature (T_s) (Pereira et al. 2009b). g_{bV} is the aerodynamic conductance (m s^{-1}) for water vapour integrated over the distance between the surface of the foliage and the adjacent air and is given by $g_{bV} = 0.07Lu^{0.441}$ (Pereira et al. 2009b), where L is the single tree leaf area index ($\text{m}^2 \text{m}^{-2}$) and u is the wind speed (ms^{-1}). Surface or canopy conductance (g_c) was assumed to be infinity, thus giving the potential evaporation – i.e. the evaporation rate from a wet canopy surface. Specifically, daily air temperature, relative humidity and wind speed were obtained from Environment Canada during the study period of December 2007 to November 2008 (Environment Canada 2015). The rainfall data, including total rainfall and duration for each event over the study period, were obtained from Asadian et al. (2009), who used tipping bucket rain gauges to measure the rainfall and throughfall of urban trees in the DNV. The value of \bar{R} was then calculated by dividing gross precipitation P_G by the duration of the rainfall event. It has been suggested that errors might be introduced by dividing P_G by the entire duration of the rainfall event, because the true rainfall rate should be the rainfall rate after the canopy is saturated (Gash et al. 1995; Valente et al. 1997). This issue will be further discussed in later sections.

The two canopy parameters p and S were estimated from the LAI of specific tree species based on the following equations:

$$c = 1 - \exp(-kL) \quad (12)$$

$$S = S_L L + S_b B \quad (13)$$

where L is the single-tree LAI. As mentioned above, p is often assumed to equal $1 - c$ (Gash et al. 1995), which was determined by its relationship to LAI (Wang et al. 2008). k is the extinction coefficient, which has a range

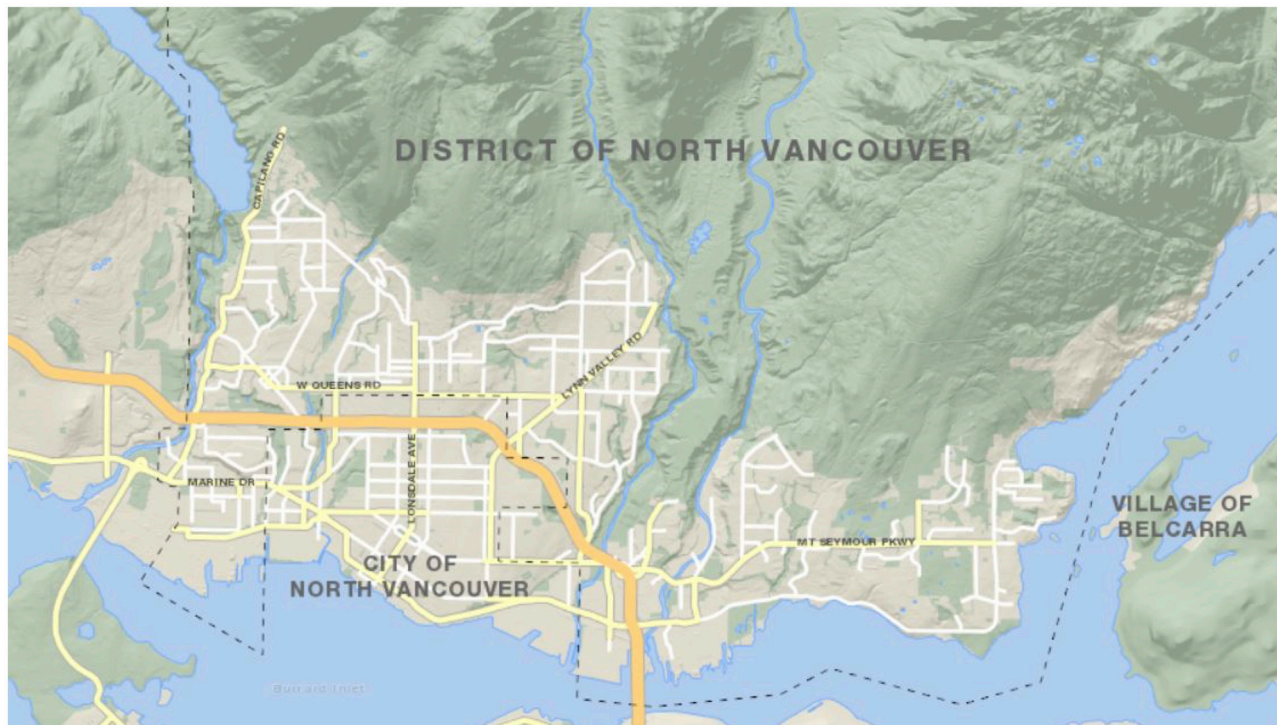


Figure 2. Map of the District of North Vancouver, BC.

between 0.6 and 0.8 (Ross 1975). A value of 0.7 was set as the default value for k in the model. As no data for local trees were available, a specific LAI for each tree species, assuming they are at their mature stage, was obtained from Nowak (1994), who provided a list of LAI values for the common street tree species in Chicago, Illinois, USA. LAI of a single tree is defined as one-sided leaf surface area divided by the ground area occupied by the plant (Nowak 1994).

S was assumed to be linearly related to LAI (Liu 1998; Wang et al. 2008). Thus, the relationship between S and LAI is expressed as in Equation (13), where S_L (m) is the specific leaf storage, which is the maximum depth of water retained by the leaves of a particular species per unit leaf area (Tobón Marin 1999). Similarly, S_b (m) is the specific bark surface storage, which is the maximum volume of water retained by the stem and trunk of a particular tree species per unit bark area, while B is the bark area index (BAI), i.e. the trunk and branch area per unit ground area (Liu 1998). The value of S_L was set to be 0.0002 m based on reported values applied in a similar study (Wang et al. 2008). Specific BAI and S_b values were obtained from Liu (1998). By plotting stemflow versus $[T - (1 - c)P_G]$, the trunk storage capacity, S_t can be estimated as the negative intercept, and the drainage partitioning coefficient p_d can be obtained as the slope of this linear regression equation divided by $(1 + \text{slope})$ (Valente et al. 1997; Price

et al. 2003). However, since no stemflow was measured in this study, the mean values for both parameters were taken from Valente et al. (1997).

The seasonal variation of LAI must also be considered, as it changes S and p . For deciduous species, LAI reaches its maximum during the summer and its minimum during winter (dominated by BAI), and experiences leaf emergence in spring and senescence in fall. For model simplification, 80% of LAI after emergence values for both spring and fall were assumed. The LAI values obtained from Nowak (1994) were assumed to be the summer values for each selected tree species, and the summer LAI values also served as the basis of spring and fall LAI calculations. Table 1 summarizes the data inputs and the sources used in the model.

Results and discussion

Model performance

Before testing the model on four selected broadleaf species, it was validated by comparing the results of modelled I with measured I . The I data for the species of interest in this study were not available; thus, I data for one Douglas-fir tree and one western redcedar tree in the urban environment of the DNV measured by Asadian et al. (2009) over a one-year period were used. The model was applied on an event basis using T vs. P_G estimated \bar{E}_c/\bar{R} (Figure 1), and the water vapour diffusion

Table 1. Summary of data inputs for the District of North Vancouver rainfall interception model.

Inputs	Outputs	Equations	Data sources
<i>Meteorological data</i>			
Air temperature (T_a , °C)	Averaged evaporation rate (\bar{E}_c)	Eq. (11)	Environment Canada: https://climate.weather.gc.ca/historical_data/search_historic_data_e.html
Relative humidity (RH, %)			
Wind speed (u , m/s)			
Gross rainfall (P_G , mm)	Averaged rainfall rate (\bar{R})	\bar{R} (mm/h) = P_G/t	Empirical measurements (Asadian and Weiler 2009)
Duration of rainfall event (t , h)			
<i>Crown parameters</i>			
LAI	c	Eq. (12) ($p = 1 - c$)	Nowak (1994)
	S (mm)	Eq. (13)	
<i>Trunk parameters</i>			
	p_d	n/a	Valente et al. (1997)
	S_t (mm)	n/a	

equation (Equation 11) with g_{bV} estimated using aerodynamic approach (Equation (22) in Valente et al. 1997) for the determination of \bar{E}_c/\bar{R} (Table 1). The aerodynamic approach was used rather than scaling up from leaf boundary layer conductance as in Pereira et al. (2009b) because it was found that using the latter approach overestimated \bar{E}_c . This appeared to be due to the difficulty in parameterizing the boundary layer conductance of the small leaves (needles) of coniferous trees and to their large LAI compared to deciduous trees. For this comparison, stemflow was considered negligible since it is a minor component of the water balance for mature canopies, especially for coniferous tree species (Asadian et al. 2009). S and p for both methods of estimating of \bar{E}_c/\bar{R} were obtained from the T vs. P_G plot. The interception loss for each of Douglas-fir and western redcedar trees was obtained by applying the same method of calculation described in the Interception Calculation section.

Figure 3 shows a comparison of the two approaches of modelled I with measured I for the two trees. Overall, the model performed relatively well, and the patterns of modelled and measured I were very similar to each other (Figure 3). The model slightly underestimated I for both approaches. More underestimation in interception loss was shown in \bar{E}_c/\bar{R} estimated using the T vs. P_G plot compared to aerodynamic approach estimated \bar{E}_c/\bar{R} for both species (Table 2). The modelled I with aerodynamic approach estimated \bar{E}_c/\bar{R} showed better agreement with the measured I with a variance (normalized averaged error) of 19% for western redcedar and 6% for Douglas-fir over the simulation period. However, the difference between the modelled I using \bar{E}_c/\bar{R} obtained from the T vs. P_G and measured I increased after April for both tree species, with a larger difference observed in the case of Douglas-fir (Table 2).

Many factors could cause differences between modelled and measured data. Differences in crown shape and leaf morphology of western redcedar and Douglas-fir lead to variations in rainfall distribution patterns and the total amount of interception. The crown shape and leaf morphology of these two species also impact the canopy storage capacity and aerodynamic conductance, which is a key variable in estimating \bar{E}_c . Other causes for the discrepancy between modelled and measured interception may result not only from canopy characteristics, but also from the variation in rainfall rates and evaporation rates. High evaporation rates in summer months and larger variances of rainfall rates in late fall and winter months impact the total interception losses for these two species. Importantly, the rainfall rate and evaporation rate should be measured specifically for complete canopy saturation conditions during a rainfall event, as the Gash model is very sensitive to these two parameters (Asdak et al. 1998; Pereira et al. 2009a). In the case of this comparison, \bar{E}_c/\bar{R} values obtained from both approaches were treated as constants over the event period rather than the period after complete saturation conditions. Assuming \bar{E}_c/\bar{R} is constant during a rainfall event may not be appropriate, especially during the wetting phase, and is potentially responsible for some errors (Link et al. 2004). Additionally, treating S and p as constants requires further estimates, as they can be affected by moisture, temperature and evaporation rate (Véliz-Chávez et al. 2014). Importantly, using a one-dimensional aerodynamic approach may not adequately estimate \bar{E}_c when the trees behave as isolated units, because the effect of under-strata on the overall aerodynamic conductance and evaporation is very different compared to closed-canopy conditions (Valente et al. 1997; Pereira et al. 2009b). Therefore, an individual tree approach, suggested by (Pereira et al. 2009b), will be applied in the following analysis of four urban tree

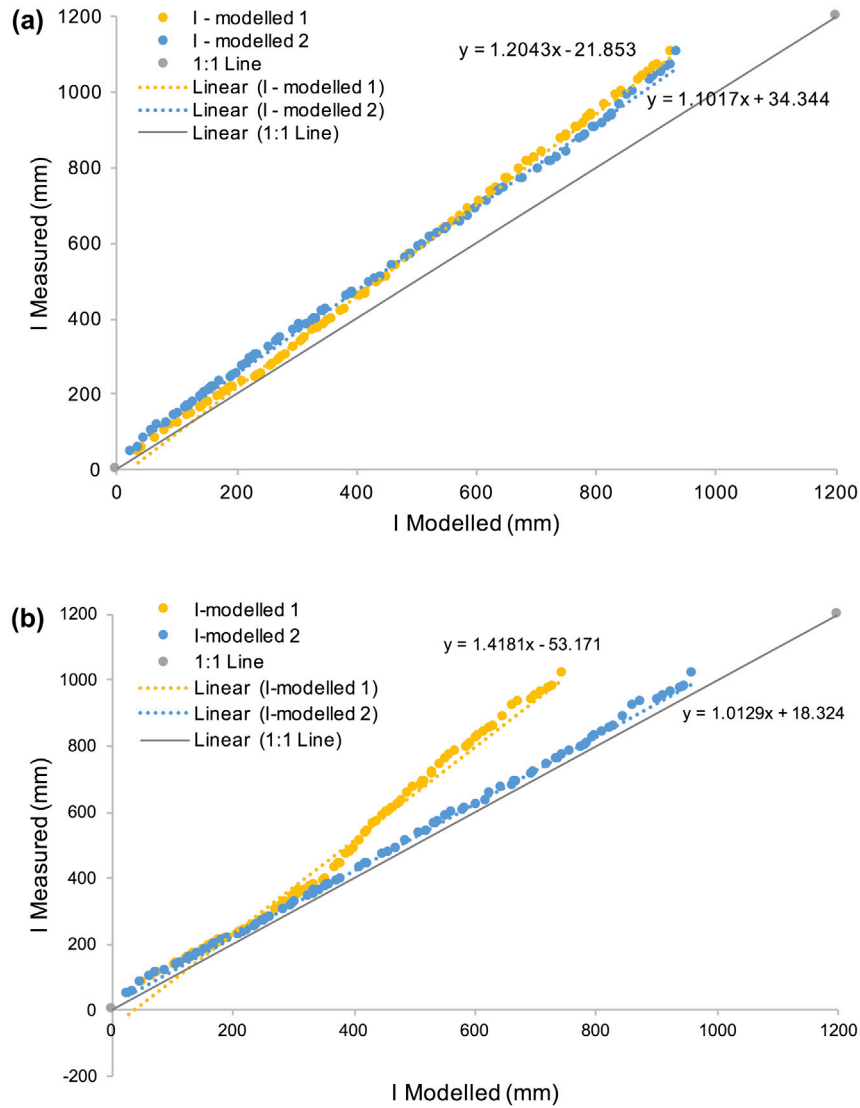


Figure 3. Comparison of measured and modelled cumulative interception (I) for two species: (a) western redcedar (WRC); (b) Douglas-fir (DF). I -modelled 1: I vs. P_G estimated using \bar{E}_c/\bar{R} ; I -modelled 2: Using Equation 11 estimated \bar{E}_c/\bar{R} with g_{vb} estimated using aerodynamic approach.

Table 2. Results of the comparison of models using two different methods (i.e. T vs. P_G relationship and diffusion equation (Equation 11) with the g_{vb} calculated using the aerodynamic approach) and measured interception for two species.

	Western redcedar		Douglas-fir	
	T vs. P_G estimated \bar{E}_c/\bar{R}	Diffusion equation estimated \bar{E}_c/\bar{R}	T vs. P_G estimated \bar{E}_c/\bar{R}	Diffusion equation estimated \bar{E}_c/\bar{R}
P_G (mm)	1474	1474	1474	1474
I (mm) measured	1108	1108	1016	1016
I (mm) modelled	926	935	746	959
Normalized averaged error (%) for modelled interception loss	19.6	18.5	36.2	5.9

species. It is emphasized that the model summarizes general conditions. Minor discrepancies are reasonable, as the measured data only represent the interception loss of one tree species for one rainfall event.

Sensitivity analysis

Although the model performance is influenced by the combination of effects of several parameters, some parameters have a greater impact than the others. An analysis of the sensitivity of I to the three major parameters in the model (i.e. S , p , and \bar{E}_c/\bar{R}) was conducted by varying the three parameter values by $\pm 10\%$, $\pm 20\%$ and $\pm 30\%$ for the model results for a white oak tree.

Among the three major parameters, \bar{E}_c/\bar{R} is the most sensitive parameter in the model (Figure 4). A similar result was found by Šraj et al. (2008), who found that a 10% change in \bar{E}/\bar{R} led to a 7% change in the modelled interception loss. Deguchi et al. (2006) reported that a 30% change in \bar{E}/\bar{R} led to a 20% change in modelled interception loss. In this analysis, a 30% decrease in \bar{E}_c/\bar{R} reduced interception loss by almost 40%, which is the largest change in this sensitivity analysis (Figure 4). It would be informative to know which one of \bar{E}_c and \bar{R} has a greater impact on the model results. Unfortunately, with the limited data currently available, it was not possible to do a detailed separation of the effects of \bar{E}_c and \bar{R} . However, by examining the effects of the maximum and minimum values of \bar{E}_c/\bar{R} , it was found that \bar{R} has a greater impact on the model than \bar{E}_c does (Figure 4). Fan et al. (2014) found that a 40% decrease in \bar{R} led to a more than 40% increment in predicted interception loss, while a 40% decrease in \bar{E} only led to about a 27%

reduction in predicted interception loss. Xiao et al. (2000) reported that I could increase from 32 to 57% with a reduction of 50% in rainfall rate for an oak tree. Decreasing rainfall rate reduced the amount of rainwater intercepted by the tree canopy, resulting in the accumulation of a large proportion of rainwater on the crown surface (Xiao et al. 2000). Additionally, I typically decreases asymptotically with P_G until reaching a quasi-constant value once a certain threshold P_G has been met; thus, I tends to be higher with lower \bar{R} (Carlyle-Moses et al. 2011).

Compared to \bar{E}_c/\bar{R} , the model showed less sensitivity to both p and S . In this study, both S and p showed similar sensitivity to the model (Figure 4), although some similar studies have suggested that S is more sensitive compared to p (e.g. Gash et al. 1978; Deguchi et al. 2006; Fan et al. 2014). Gash et al. (1978) reported that a change of 50% in S led to a variation of 15% in I , while a change of 50% in p led to only 7% variation in I . Similar results were reported by Deguchi et al. (2006) and Fan et al. (2014), who found that a change of 10% in I resulted from a change of 30–40% in S , while about 5% change in I was observed for the same percentage change in p . Higher impacts of S compared to p were also reported by Šraj et al. (2008), who indicated a 10% change in S resulted in a change of 1.4% in modelled I , and only 0.8% for the same percentage change in p . The influences of canopy parameters are restricted to the period of canopy wetting-up and to the amount of water left on the canopy after rainfall has ceased (Gash et al. 1978). Low sensitivity of canopy parameters in this analysis could also reflect the rainfall and evaporation characteristics over this study period.

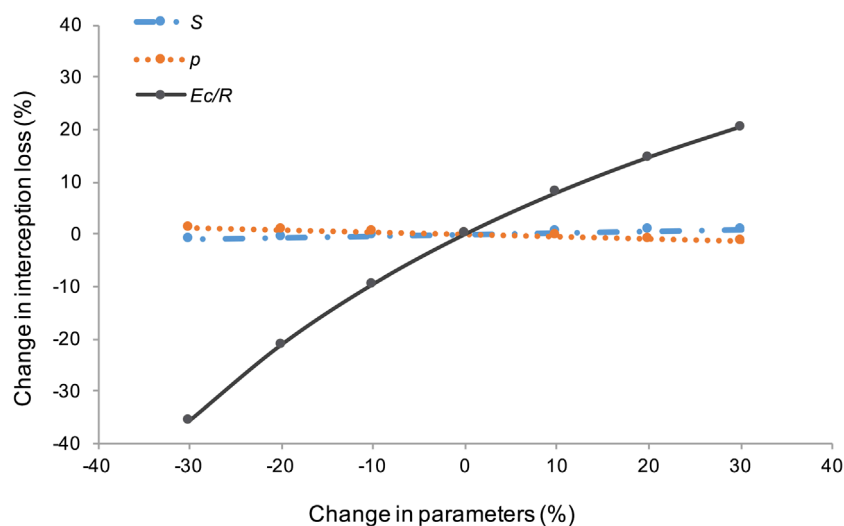


Figure 4. Analysis of sensitivity of I to changes in (a) \bar{E}_c/\bar{R} , (b) p , and (c) S with changes of $\pm 10\%$, $\pm 20\%$ and $\pm 30\%$ applied on the model results for a white oak tree.

Application to four deciduous tree species

The previous section demonstrated that the model is an effective tool to estimate interception loss. To see how the interception losses vary among deciduous trees, it is useful to test the model against the tree species that are grown in local municipalities. The interception loss was calculated by applying Equations (4) to (8). The Pereira et al. (2009b) approach was employed in \bar{E}_c to estimate with small modifications made on aerodynamic conductance (g_{bv}) by selecting an appropriate LAI and adjusting the coefficient 0.06 in Equation (7) of Pereira et al. (2009b) based on the leaf width for the species of interest, based on Schuepp (1993). The tree selection was determined by a simple survey conducted in several municipalities including DNV within Metro Vancouver area. White oak (*Quercus alba* L.), Norway maple (*Acer platanoides* L.), green ash (*Fraxinus pennsylvanica* Marsh.) and *Prunus* sp. were found to be the most common planted street tree species in the urban region and therefore were selected for testing the rainfall interception model.

The climate data from December 2007 to November 2008 are shown in Figure 5. These data were acquired from the climate station located at Vancouver International Airport, British Columbia (Environment Canada 2015). Data show that the highest amount of precipitation occurred during November and March in 2008, and the highest mean daily temperatures were observed in the months of July and August. For this analysis, the seasons were divided into winter (December, January, February), spring (March, April, May), summer (June, July, August) and fall (September, October, November).

Because all four species lose their leaves during winter, the storage of water was dominated by stem and

branches accounting for almost zero I in winter. Thus, the rainfall interception losses were assumed to be the same for all selected species in the winter months (Figure 6(a)). The cumulative rainfall intercepted by each species diverged in March and April, following the start of leaf emergence. Among the four species, white oak showed the highest capacity of interception through the whole study period, followed in decreasing order by Norway maple, green ash and *Prunus* sp., and only small differences were observed between green ash and *Prunus* sp. Higher interception loss can be attributed to larger canopy storage capacity and larger aerodynamic conductance (Valente et al. 1997). Differences in water storage capacities among these species reflected the differences in the morphogenesis of leaf surfaces, which influence the surface water storage, by affecting the amount of throughfall and drop size (Xiao et al. 2016). Variations in leaf size also influence the evaporation rate by affecting the aerodynamic conductance (Pereira et al. 2009b). Other factors that vary among species, such as leaf hydrophobicity, roughness, geometry and inclination, also have impacts on the water storage capacity of the leaf surface (Nanko et al. 2006, 2013). Despite the differences among species, the patterns of cumulative interception loss for each species are very similar to each other until the late summer, when divergence among species is observed.

Figure 6(b) shows averaged interception loss, per event, on a monthly basis for each species. All four species exhibited a similar monthly pattern of interception loss. In general, a high peak for all species was observed in summer months, and the lowest interception loss was observed in the winter months, when very little rainfall

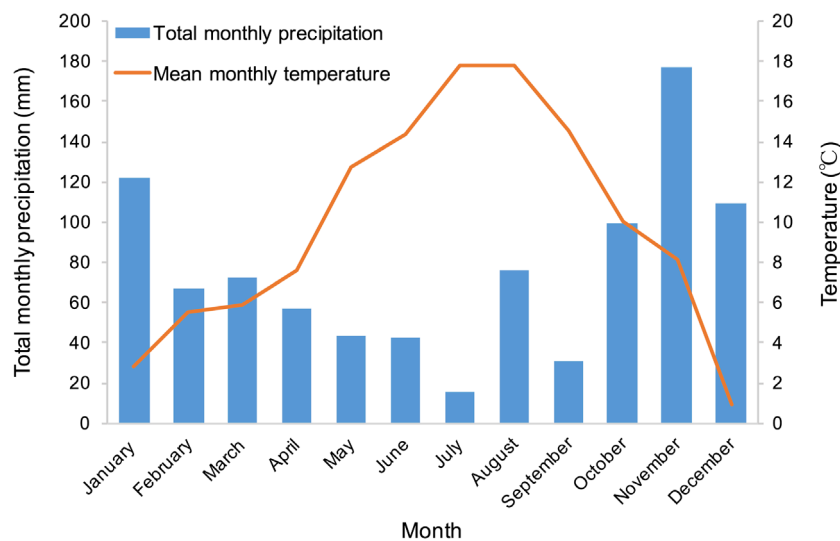


Figure 5. Vancouver's Climate Data from December 2007 to November 2008 Vancouver International Airport (location of rain gauge: latitude 49°11'42N; longitude: 123°10'55W).

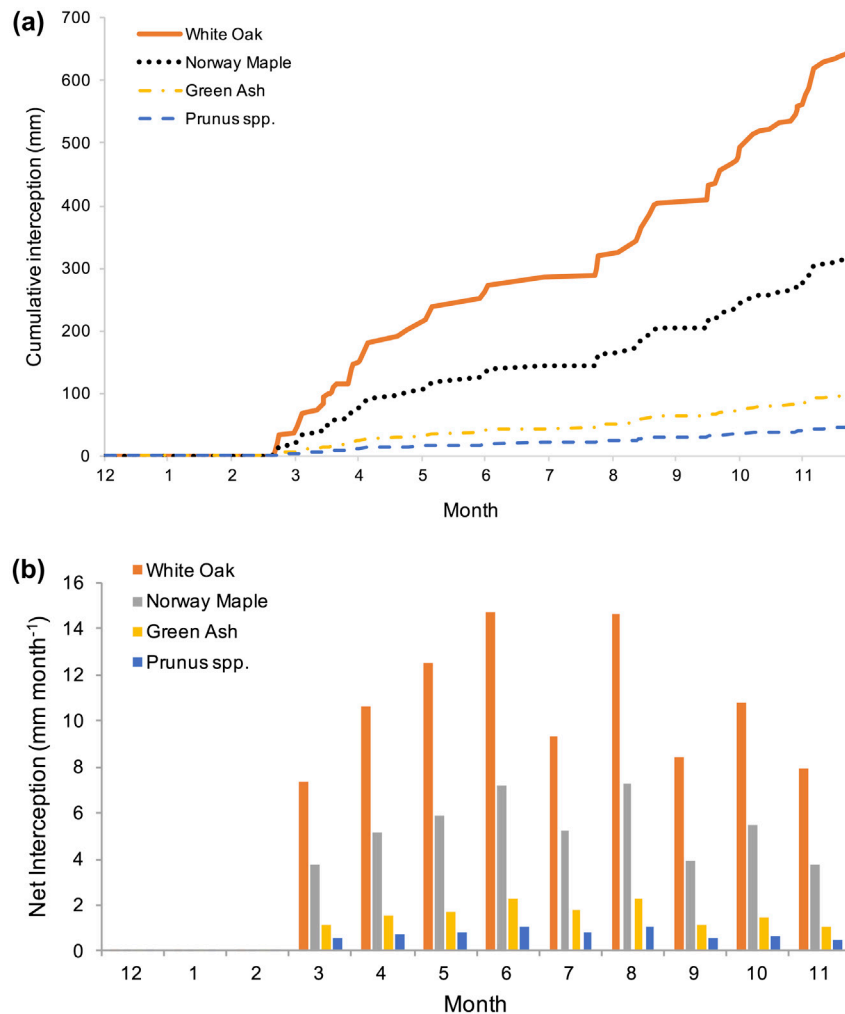


Figure 6. Seasonal interception loss of four tree species (white oak, Norway maple, green ash and *Prunus* sp.), presented as: (a) cumulative sum of interception loss, and (b) monthly averaged interception loss for each rain event.

was intercepted by the stem and the branches for all species. The average interception loss for each rainfall event started in March at 7.38 mm and 3.78 mm for white oak and Norway maple, respectively (highest of the four species), and gradually increased over time. The highest interception loss for all species was observed in June. High interception loss per rainfall event during summer could be explained by the high evaporation rate resulting from high air temperature and vapour pressure deficit. It is evident that annual patterns of air temperature (Figure 5) and average interception loss (Figure 6(b)) are similar during spring and early summer, but variations were observed in late summer and fall. The amount of rainfall received in fall and winter in the Vancouver area is high, with larger variation in rainfall rates compared to that in spring and summer. Moreover, for seasons dominated by a series of relatively small rainfall events, I may be large, whereas I may be comparatively small if the most of P_G falls during relatively large events,

because I typically decreases asymptotically with P_G until reaching a quasi-constant value once a certain threshold of P_G has been met (Carlyle-Moses et al. 2011).

Total stemflow estimated from this analysis ranged from 0.01% (Norway maple) to 0.04% (white oak) of total precipitation. As shown by Valente et al. (1997), stemflow is the difference between I_{ts} and I_t in Equations (6) and (7), respectively. This assumes that water is diverted to the trunks only after the canopy is saturated, and stemflow is generated only when the trunk is saturated (Gash et al. 1995; Valente et al. 1997). Also, a high evaporation rate will result in lower stemflow as water evaporates before stemflow initiation. Two trunk-related parameters (i.e. p_{db} , S_t) play an important role in a better estimation of stemflow. David et al. (2006) showed that stemflow only represents 0.26% of gross rainfall for *Quercus ilex* on a crown area basis. Šraj et al. (2008) reported that stemflow values were

4.5% for an ash tree plot and 2.9% for an oak tree plot. However, a high percentage of stemflow was found in some isolated trees in urban environments. Schooling et al. (2015), for example, found that the event maximum stemflow percentage was 22.8% for a columnar English oak. Tree characteristics such as height, diameter at breast height (DBH), bark texture, branch angle and overlapping of tree crowns could all affect the volume of stemflow (Deguchi et al. 2006; Šraj et al. 2008; Schooling et al. 2015). It has been recognized that stemflow from urban trees promotes infiltration and diverts precipitation from becoming stormwater runoff (Schooling et al. 2015). Given its hydrological importance in urban environments, stemflow should be considered in future urban rainfall partitioning studies.

In this study, \bar{E}_c/\bar{R} , S and p were assumed to be constant over the whole rainfall event. This assumption could lead to the discrepancy between modelled and measured I discussed in the 'Model performance' section. In fact, both \bar{E}_c and \bar{R} should correspond to the period after the tree canopy is completely saturated. Another limitation was that LAI values were taken for the same species of mature trees from a different study area. LAI varies in different environments, even for the same tree species. For example, various types of land use could lead to different LAI values for the same species (Nowak et al. 2013). Deviation in LAI could cause biases in the estimation of both S and p in the model. Furthermore, variations in leaf phenology of different species should be considered. Leaf phenology determines the timing of the emergence of leaves, the growth of leaves and leaf senescence (Rodriguez et al. 2014). The leaf-on season was assumed to be spring, summer and fall, and the leaf-off season was assumed to be winter, for all broadleaf species. This could have affected somewhat the cumulative amount of interception loss for different species. While \bar{R} is an important model parameter it was not possible to estimate it, although it was found that \bar{E}_c/\bar{R} was slightly more influential than \bar{E}_c . The model is expected to assist in tree species selection regarding rainfall interception capacity, which would offer options for developers and landscape architects in selecting specific tree species to meet various goals. It is recommended that the effects of wind direction and tree crown shape on interception losses also be considered in future research.

Conclusions

Overall, the model performed well in simulating canopy interception loss. The discrepancies between modelled values and observations could be attributed to uncertainty in the measurements of air temperature, wind speed, relative humidity, leaf area index and rainfall rate. The lack of the corresponding ratio of the average

evaporation rate (\bar{E}_c) to the average rainfall rate (\bar{R}) when the canopy is saturated may introduce errors when applying the model. The sensitivity analysis indicated the significant effect of \bar{E}_c/\bar{R} on the model performance with little sensitivity to variations in crown storage (S) and the free throughfall coefficient (p). Separating the impacts of evaporation rate and rainfall rate would require more detailed analysis. The effects of inter-species variation on interception was evident, as white oak showed the highest interception loss in both cumulative values and monthly average values for each rainfall event, followed by Norway maple, green ash and *Prunus* sp. There is a need for species-specific empirical data to further improve the model.

Acknowledgements

The authors wish to acknowledge the valuable contributions provided by Andreas Christen (Geography Department, UBC), Richard Boase (Environmental Officer, District of North Vancouver), Hans Schreier and Julie Wilson (Master of Land and Water Systems programme, UBC). We thank two anonymous reviewers for comments that helped us to greatly improve the manuscript.

References

- Asadian Y. and M. Weiler. 2009. A new approach in measuring rainfall interception by urban trees in coastal British Columbia. *Water Quality Research Journal of Canada* 44 (1): 16.
- Asdak C. P. G. Jarvis and P. V. Gardingen. 1998. Modelling rainfall interception in unlogged and logged forest areas of Central Kalimantan, Indonesia. *Hydrology & Earth System Sciences* 2 : 211–220.
- Bryant M. L. S. Bhat and J. M. Jacobs. 2005. Measurements and modeling of throughfall variability for five forest communities in the southeastern US. *Journal of Hydrology* 312: 95–108. doi:doi.org/10.1016/j.jhydrol.2005.02.012.
- Carlyle-Moses D. E. and J. H. C. Gash. 2011. Rainfall interception loss by forest canopies. In *Forest hydrology and biogeochemistry*, eds. D.F. Levia, D. Carlyle-Moses, and T. Tanaka, 407–423. Netherlands: Springer.
- Carlyle-Moses D. E. and J. T. Schooling. 2015. Tree traits and meteorological factors influencing the initiation and rate of stemflow from isolated deciduous trees. *Hydrological Processes* 29 (18): 4083–4099. doi:10.1002/hyp.10519.
- David, T. S., J. H. C. Gash, F. Valente, J. S. Pereira, M. I. Ferreira, and J. S. David. 2006. Rainfall interception by an isolated evergreen oak tree in a Mediterranean savannah. *Hydrological Processes* 20 (13): 2713–2726.
- Deguchi A. S. Hattori and H. T. Park. 2006. The influence of seasonal changes in canopy structure on interception loss: application of the revised gash model. *Journal of Hydrology* 318 (1): 80–102. doi:10.1016/j.jhydrol.2005.06.005.
- Environment Canada. 2015. Historical data. https://climate.weather.gc.ca/historical_data/search_historic_data_e.html (accessed June 2016).
- Fan J. K. T. Oestergaard A. Guyot and D. A. Lockington. 2014. Measuring and modeling rainfall interception losses by a native Banksia Woodland and an exotic pine plantation in subtropical coastal Australia. *Journal of Hydrology* 515: 156–165. doi:10.1016/j.jhydrol.2014.04.066.

- Gash J. H. C. 1979. An analytical model of rainfall interception by forests. *Quarterly Journal of the Royal Meteorological Society* 105 (443): 43–55. doi:10.1002/(ISSN)1477-870X
- Gash J. H. C. and A. J. Morton. 1978. An application of the Rutter model to the estimation of the interception loss from Thetford Forest. *Journal of Hydrology* 38 (1–2): 49–58. doi:org/10.1016/0022-1694(78),90131-2.
- Gash J. H., C. R. Lloyd and G. Lachaud. 1995. Estimating sparse forest rainfall interception with an analytical model. *Journal of Hydrology* 170 (1–4): 79–86. doi:org/10.1016/0022-1694(95)02697-N.
- Klaassen W. F. Bosveld and E. de Water. 1995. Water storage and evaporation as constituents of rainfall interception. *Journal of Hydrology* 212–213: 36–50. doi:10.1016/S0022-1694(98)00200-5.
- Leyton L. E. R. C. Reynolds and F. B. Thompson. 1967. Rainfall interception in forest and moorland. In *International symposium on forest hydrology*, eds. W.E. Sopper and H.W. Lull, 163–168. New York: Pergamon Press.
- Link T. E. M. Unsworth and D. Marks. 2004. The dynamics of rainfall interception by a seasonal temperate rainforest. *Agricultural and Forest Meteorology* 124 (3–4): 171–191. doi:10.1016/j.agrformet.2004.01.010.
- Liu S. 1998. Estimation of rainfall storage capacity in the canopies of cypress wetlands and slash pine uplands in North-Central Florida. *Journal of Hydrology* 207 (1–2): 32–41. doi:10.1016/S0022-1694(98)00115-2.
- Livesley S. J. G. M. McPherson and C. Calfapietra. 2016. The urban forest and ecosystem services: impacts on urban water, heat, and pollution cycles at the tree, street, and city scale. *Journal of Environment Quality* 45 (1): 119. doi:10.2134/jeq2015.11.0567.
- McPherson E. G. and J. R. Simpson. 2002. A comparison of municipal forest benefits and costs in Modesto and Santa Monica, California. *USA. Urban Forestry & Urban Greening* 1 (2): 61–74. doi:10.1078/1618-8667-00007
- McPherson E. G. N. van Doorn and J. de Goede. 2016. Structure, function and value of street trees in California, USA. *Urban Forestry and Urban Greening* 17 : 104–115. doi:org/10.1016/j.ufug.2016.03.013.
- Murakami S. 2007. Application of three canopy interception models to a young stand of Japanese cypress and interpretation in terms of interception mechanism. *Journal of Hydrology* 3–4: 305–319. doi:10.1016/j.jhydrol.2007.05.032.
- Nanko K., N. Hotta and M. Suzuki. 2006. Evaluating the influence of canopy species and meteorological factors on throughfall drop size distribution. *Journal of Hydrology* 329 (3–4): 422–431. doi:10.1016/j.jhydrol.2006.02.036.
- Nanko K. A. Watanabe N. Hotta and M. Suzuki. 2013. Physical interpretation of the difference in drop size distributions of leaf drips among tree species. *Agricultural and Forest Meteorology* 169: 74–84. doi:10.1016/j.agrformet.2012.09.018.
- Nowak D. J. 1994. Urban forest structure: the state of Chicago's urban forest. Chap. 2 in *Chicago's urban forest ecosystem: results of the Chicago Urban Forest Climate Project Report NE-186*, ed. G. E. McPherson D. J. Nowak and R. A. Rowntree, 3–18. Washington, DC: USDA Forest Service, Northeastern Forest Experiment Station.
- Nowak, D. J. R. E. I. Hoehn A. R. Bodine D. E. Crane J. F. Dwyer V. Bonnewell and G. Watson. 2013. Urban Trees and Forests of the Chicago Region. *U.S. Forest Service* 114 p.
- Peper P. J. E. G. McPherson J. R. Simpson S. L. Gardner K. E. Vargas and Q. Xiao. 2007. *New York city, New York municipal forest resource analysis*. New York: Center for Urban Forest Research, USDA Forest Service, Pacific Southwest Research Station.
- Pereira F. L. J. H. C. Gash J. S. David T. S. David P. R. Monteiro and F. Valente. 2009a. Modelling interception loss from evergreen oak Mediterranean savannas : Application of a tree-based modelling approach. *Agricultural and Forest Meteorology* 149: 680–688. doi:10.1016/j.agrformet.2008.10.014.
- Pereira F. L. J. H. C. Gash J. S. David and F. Valente. 2009b. Evaporation of intercepted rainfall from isolated evergreen oak trees: Do the crowns behave as wet bulbs? *Agricultural and Forest Meteorology* 149 (3): 667–679. doi:10.1016/j.agrformet.2008.10.013.
- Price A. G. and D. E. Carlyle-Moses. 2003. Measurement and modelling of growing-season canopy water fluxes in a mature mixed deciduous forest stand, Southern Ontario. *Canada. Agricultural and Forest Meteorology* 119 (1): 69–85. doi:10.1016/S0168-1923(03)00117-5.
- Rodriguez H. G., R. Maiti and N. C. Sankar. 2014. Phenology of woody species: a review. *International Journal of Bio-Resource and Stress Management* 5 (3): 436. doi:10.5958/0976-4038.2014.00595.8.
- Ross J. 1975. Radiative transfer in plant communities. *Vegetation and the Atmosphere* 1: 13–55.
- Schooling J. T. and D. E. Carlyle-Moses. 2015. The influence of rainfall depth class and deciduous tree traits on stemflow production in an urban park. *Urban ecosystems* 18 (4): 1261–1284. doi:10.1007/s11252-015-0441-0.
- Schuepp P. H. 1993. Tansley review no. 59 leaf boundary layers. *New Phytologist* 125 (3): 477–507.
- Šraj M. M. Brilly and M. Mikoš. 2008. Rainfall interception by two deciduous Mediterranean forests of contrasting stature in Slovenia. *Agricultural and Forest Meteorology* 148 (1): 121–134. doi:10.1016/j.agrformet.2007.09.007.
- Tobón Marin C. 1999. Monitoring and modelling hydrological fluxes in support of nutrient cycling studies in Amazonian rain forest ecosystems. *Tropendos Series* No. 17.
- Valente F. J. S. David and J. H. C. Gash. 1997. Modelling interception loss for two sparse eucalypt and pine forests in central Portugal using reformulated Rutter and Gash analytical models. *Journal of Hydrology* 190 (1–2): 141–162.
- Véliz-Chávez C. C. A. Mastachi-Loza E. González-Sosa R. Becerril-Piña and N. M. Ramos-Salinas. 2014. Canopy storage implications on interception loss modeling. *American Journal of Plant Sciences* 5 (20): 3032–3048.
- Wang J. T. A. Endreny and D. J. Nowak. 2008. Mechanistic simulation of tree effects in an urban water balance model. *Journal of the American Water Resources Association* 44 (1): 75–85. doi:10.1111/j.1752-1688.2007.00139.x.
- Water Balance Model Express. 2016. Welcome to the district of North Vancouver water balance tool. <https://dvn.waterbalance-express.ca> (accessed August 2016).
- Xiao Q. and E. G. McPherson. 2003. Rainfall interception by Santa Monica's municipal urban forest. *Urban Ecosystems* 6 (4): 291–302.
- Xiao Q. and E. G. McPherson. 2016. Surface Water Storage Capacity of Twenty Tree Species in Davis. *California. Journal of Environmental Quality* 45 (1): 188–198. doi:10.2134/jeq2015.02.0092.
- Xiao Q. E. G. McPherson S. L. Ustin and M. E. Grismer. 2000. A new approach to modeling tree rainfall interception. *Journal of Geophysical Research* 105 (D23): 29–173.